# Collapses of underground cavities and soil-structure interactions: experimental and numerical models

Matthieu Caudron, Fabrice Emeriault, Richard Kastner, Marwan Al Heib

# Collapses of underground cavities and soil-structure interactions : Experimental and numerical models.

**M. CAUDRON*, F. EMERIAULT, R. KASTNER**
URGC Géotechnique, INSA de Lyon, 34 Avenue des Arts, 69621 VILLEURBANNE Cedex FRANCE
*Corresponding author; e-mail : matthieu.caudron@insa-lyon.fr

**M. AL HEIB**
INERIS, Ecoles de Mines – Parc de Saurupt, 54042 NANCY Cedex, FRANCE

**Abstract :** In this paper, soil-structure interaction during a sinkhole phenomenon is studied by a dual approach using a physical model and a numerical method. First of all, the physical model will use the bidimensionnal Schneebeli material in a small-scale model allowing fully controlled test conditions. The Schneebeli material is modified in order to exhibit a cohesive frictional behaviour. The soil mass of average dimensions (0.75m wide and up to 0.50m high) makes it possible to represent a sinkhole with a scale factor of 1/40. The use of a building model will allow us to shed some light on the soil-structure interaction during the sinkhole.

**Keywords** : sinkhole, soil-structure interaction, physical model, numerical model.

## 1 Objectives

The great subsidences result from the collapses of underground cavities, whether man-made or formed naturally by water flow in soluble solid mass of rocks. Recent studies [DECK et al., 2002][VEZOLE, 2002] show the various impact of such phenomenon on the existing structure standing on the surface. We will study these phenomena in order to determine the impacts on the buildings.
An experimental model using an analogical soil will give us some qualitative results. Then a numerical method using a coupled approach will be setup with these results. The following step would be to study the influence of various parameters but it is not the purpose of this paper.

## 2 The physical model

The physical model used is composed of a rigid steel U shape frame that will receive the soil mass. It comprises a device inspired from the work of NAKAI [NAKAI et al., 1997]. It allows creating the cavity in a controlled way with different steps. Ten small pieces can be moved down in order to open step by step the cavity until the failure is reached.

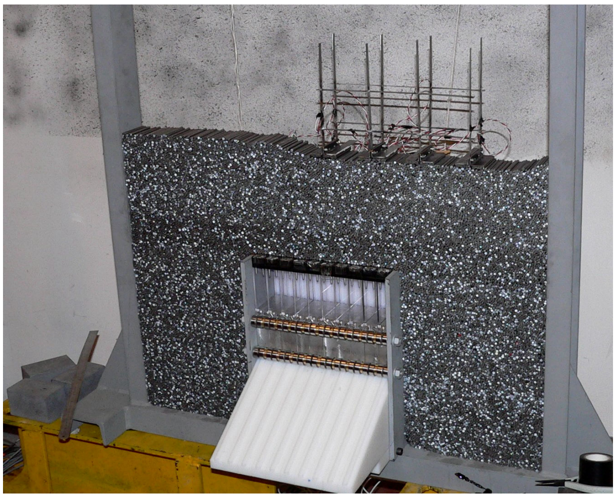

Fig. n°1 : The test bed with the apparatus to create the cavity in white and a building model.

Each moving pieces is equipped with a small force sensor in order to measure the variations of the forces applied by the soil mass on this apparatus. These sensors are connected to a computer which checks their states at given time.
To follow the movements in the soil mass, a digital camera connected to the same computer takes photos of the whole thing (test bed, soil mass and the building model when used). Theses photos are then used by a digital imagery software (Particle Imagery Velocimetry – Digital Image Correlation), developed in INSA de Lyon, in the LAMCoS laboratory [TOUCHAL et al. 1997]. The precision of this method is close to 1/100 pixel in very good conditions. WHITE [WHITE et al., 2003] showed clearly the pros and the cons of such method against the photogrammetry. With the present apparatus and test conditions, the precision is around 1/20 pixel. This corresponds to 20µm for a single couple of photos (0.8mm in real scale), very sufficient for our study.
The scale factor used for the different tests is the same one : 1/40 for the length. It may cause some problems with the interactions between the metallic rods and the structure due to the size of the rods, but the purpose of this study is to observe the qualitative aspect of the phenomenon. The rods are in stainless steel, thus the volumetric mass of the analogical soil is $65kN/m^3$. The scale factor for the mass is then 3. Given all the different relations between the scale factors to follow the laws of similarity [DEHOUSSE et ARNOUD, 1971] [BAZANT, 2004], it appears that the scale factor for the stress and for the stiffness must be 3/40.

### *2.1 The test bed*

The width of the cavity that can be simulated is at least 25mm, up to 250mm by 10 steps of 25mm (1m to 10m in real scale). Its height can be 25, 50, 75 or 100mm (1 to 4m in real scale), chosen before the beginning of the test. The figure 1 shows the apparatus used to simulate the creation of the cavity.

### *2.2 The analogical soil*

We use a SCHNEEBELI [SCHNEEBELI, 1956] material composed of 3 different sizes : 3, 4 and 5mm of diameter. A full presentation of this analogical soil can be found in

DOLZHENKO [2002].
To observe the formation of a sinkhole, at least one layer in the soil mass must be cohesive. It was achieved by soaking the concerned rods in an aqueous solution of glue. Then the soaked rods are put on the test bed and dried until complete dehydration. Two different materials can then be employed on the test bed. Their characteristics are presented in the table 1.
The dimensions of the different layers in the soil mass are presented in the table 2.

| | *Density* | *E (MPa)* | *φ (°)* | *c (kPa)* |
|---|---|---|---|---|
| Basic soil | 2.2 | 50 to 100 | 22-24 | 0 |
| Cohesive soil | 2.2 | 50 to 100 | 27-30 | 100 |

Table 1 : Characteristics of the two materials corresponding to full scale values.

| | *Thickness* | *Width* | *Position* |
|---|---|---|---|
| Basic soil | 15cm [6m] | 75cm [30m] | top |
| Cohesive soil | ~5cm [2m] | 75cm [30m] | above the cavity |

Table 2 : Geometrical characteristics of the soil mass, full scale dimensions between brackets.

## 2.3 The building model

It was defined in order to meet the laws of similarity imposed by the use of the analogical soil. Mainly its stiffness and its dimensions follow the scale factors. We know that it is quite difficult to get a good small-scale model to study the failure. The building model is designed to represent a simple structure with elastic behaviour but with deformation much more important than a real building. This allows studying the soil-structure interactions in a qualitative way. The figure 2 illustrates a representation of the structure used. It has 3 spans, an under floor space, a ground floor and a first floor. Small metallic masses are put on every floor in order to get a weight for the structure close to the real one, taking account of the scale factor.

The sole of the foundations are put under 15mm of soil (60cm in full scale, near the frost level).
The structure is equipped with strain gauges and with displacement sensors (4 LVDT), one on each sole. They are connected to the same computer used for the force sensors.

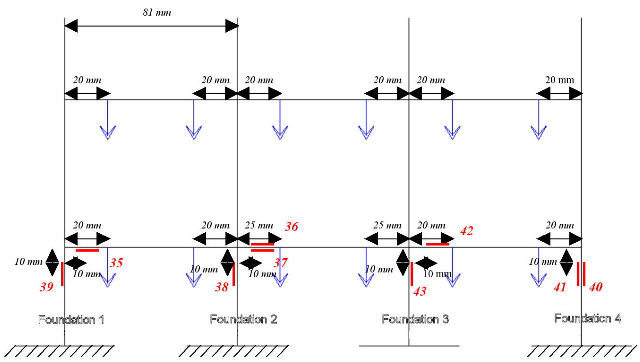


Fig. n°2 : The building model.

## 2.4 The different tests

Two different tests were carried out. The first one corresponds to green field condition. The cavity was created by moving the concerned pieces in five steps. Then a stable cavity is obtained, whose dimensions are 250mm in width and 50mm in height (10m by 2m in full scale). No visible displacements could be noted, only the digital imagery allows to measure the very small deformations after the test.
Then some water is added drop by drop in very small quantity, on the center of the cavity roof. The purpose was to weaken this area until the failure is obtained. The beginning sinkhole increases towards the top of the cohesive layer, until obtaining the complete failure of the cavity (Fig. 3).

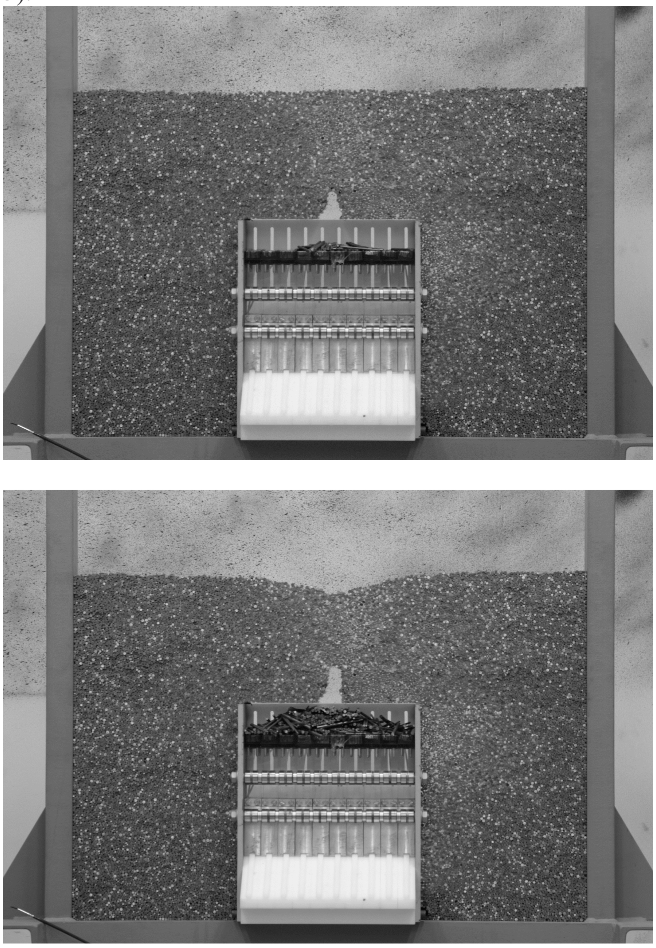

Fig. n°3 : Photos showing the beginning of the sinkhole (up) and the subsidences on the surface (down).

The second test is performed in the same conditions; the only difference is the building model standing on the soil surface. The same procedure is used to create the cavity and to get the failure. The structure stands on the ground such as the left foundation is directly above the center of the cavity (Fig. 1).

## 2.5 The main results

Firstly, with the green field test, no important movements on the ground surface are noticeable before the weakening of the cohesive layer, even when the cavity is wide open. The digital imagery process allows determining a maximal movement of 0.2mm during these different steps.
When the sinkhole is initiated by adding some water in the cohesive soil, the movement begins to appear until the complete failure of the cavity. At the end of the test, the failure of the cavity is not complete : only the left part of the cohesive layer had broken and felt into the cavity. The right part is still overhanging.
The figure 4 shows the two main stages where important subsidences reach the top of the soil mass.

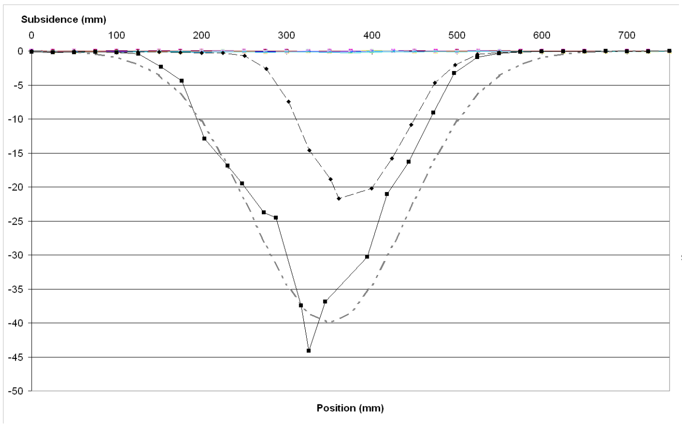


Fig. n°4 : Green field test, vertical surface movements during the two last steps and the Peck curve.

The maximum settlement is approximately 44mm (1,76m in full scale). It is very close to the height of the cavity. The width of the subsidence trough is 450mm (18m in full scale). If we try to apply the Peck formula [DOLZENKHO, 2002] to this cavity by considering a circular equivalent cavity (see [CAUDRON et al., 2004]), we get the « Peck curve » plotted on figure 4. There is no important difference with the experimental result.

$$S = S_{\max} \times e^{\left(\frac{-x^2}{2i^2}\right)} \qquad \text{(Peck Formula)}$$

Thus the forecast of the soil subsidence in green field conditions is quite satisfying in spite of the difference of failure.
The results obtained for the test with the building model are quite different. First, the failure of the cavity was more sudden. Secondly the failure mechanism is not the same: both parts of the cohesive layer break and fall into the cavity. The figure 5 illustrates the difference in both cases.

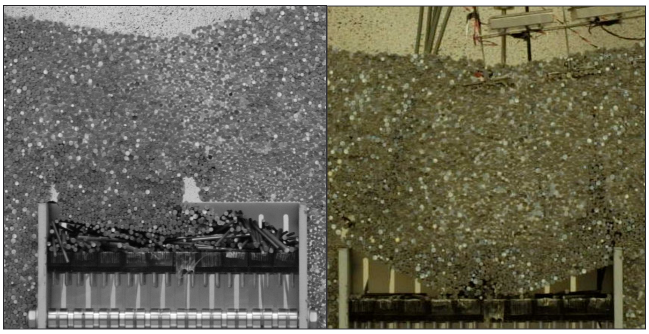

Fig. n°5 : Difference of failure for both tests (partial failure on the left, complete failure on the right).

As a result and partially due to the building model, the shape of the subsidence trough is different. Its area is wider and more asymmetric. The figure 6 shows the subsidences observed for the two tests at the same step.
The maximum vertical movement is 28% smaller than with the building. On the contrary, the width of the concerned area is 26% more important. But the volume of the trough is similar for both tests : respectively 443cm$^3$ in green field and 481cm$^3$ with the building.
The last point, but not the less important, is the maximum slope. The difference between the two tests is important : 24.7% for the green field test and 17.9% with the building. Even though in both cases it would be very damageable for a building, these tests show that it could be very cost effective to consider the soil-structure interactions when studying the effect of a sinkhole or similar phenomenon on a building.
If the relative settlements are more finely observed, it would appear that the deformations in the structure are very different as shown in the table 3.

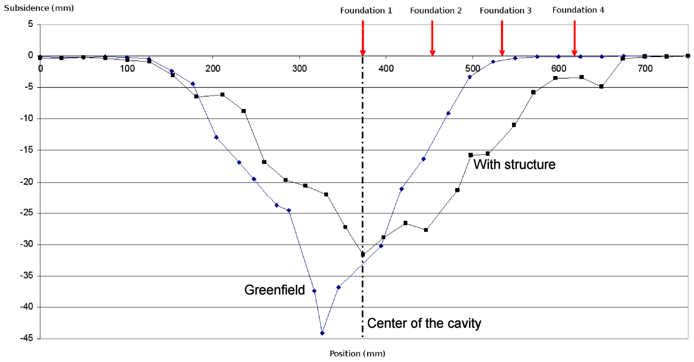


Fig. n°6 : Comparison of the subsidences between the tests in green field and with the building model (the arrows represent the position of the four foundations).

| *Span n°* | *Slope in green field* | *Slope with SSI* |
|---|---|---|
| 1-2 | 24.7% | 5.1% |
| 2-3 | 23.5% | 17.9% |
| 3-4 | 1.2% | 12.3% |

Tab n°3 : Comparison of the slopes for the three different spans named by the number of the two foundations delimiting them.

The approach commonly employed (the displacement in green field are applied directly on the building) would consider too much important deformations and moreover on the wrong place compared to the results given by the soil-structure interactions approach.

# 3 The numerical model

The computation was done using a coupled approach with FLAC$^{2D}$ and PFC$^{2D}$. The Particles Flow Code (PFC) is used to model the soil above the cavity, where large displacements should be observed. FLAC is used everywhere else a continuum approach would be satisfying. The figure 7 shows the two different regions with their respective mesh.
The model uses the same dimensions as the experimental tests : 75cm wide and 50cm high.
The FLAC grid has a U shape. Some elements of the corresponding mesh can be removed during the simulation in order to represent the creation of the cavity. The same steps are used in the numerical model than those used in the experimental test.
For FLAC, the constitutive law chosen is elastic linear due to the fact that only small deformation would be observed.

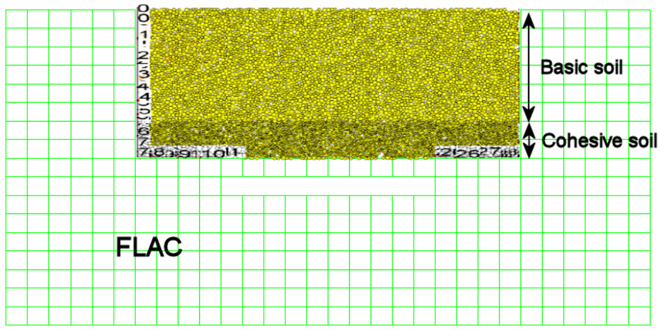


Fig. n° 7: Coupled approach with FLAC and PFC.

The PFC particles present a cohesive frictional law controlled by micro-parameters such as volumetric mass, normal and tangent stiffness, friction, ... The characteristics of the global behaviour, like E, ν, φ, c, ψ, respectively the stiffness, the Poisson coefficient, the friction angle, the cohesion and the dilatancy angle, can not be directly determined from the local parameters. Therefore several biaxial tests were performed in order to determine the best set of micro-parameters for the particles representing both cohesive and frictional analogical soils.
Once this is done, the following steps are applied to get the basic numerical model:

- Generate the particles assembly in PFC and reach stabilization.
- Create the FLAC grid, modify it as specified and reach the initial stress conditions under gravity.
- Set the coupling fishcalls between FLAC and PFC and make the whole system stabilize.
- Create the cohesion in the specified PFC region by adding contact bonds (in our case, the 5cm layer above the cavity).Stabilization.
- Create the cavity step by step by removing the corresponding mesh in FLAC.
- When the full width is reached (250mm), a procedure to weaken the cohesive layer is applied. The bonds located in the middle of the cavity roof have their strength reduced in order to simulate the effect of the water used in the experimental tests. Several steps are necessary until the failure happens.
- When the collapse is complete and stabilized, different characteristics are measured to compare the results with the physical model.

Results are only presented for greenfield conditions.

# 4 Observations

The results from the FLAC-PFC model will be compared with those from the physical model. Figure 8 shows the state of the subsidences at different computation steps:

1. The model is stable (initial state).
2. The cavity is wide open but the hard soil horizon is stable.
3. The failure is initiated by degrading the bond properties.
4. The failure is complete and large subsidences appear on the surface.

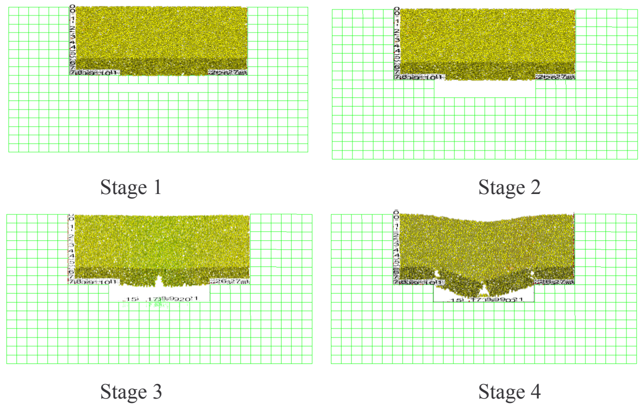


Fig. n°8 : Different snapshots of the numerical model.

Two main states can be used to compare these results with the corresponding one in the experimental test.
The first one will be the last step observed before the degradation of the hard soil layer. The main characteristics observed are the maximum displacement on the ground surface, the maximum deflection on the roof of the cavity and the development of the stress in the soil mass when the cavity is created.
The second state is the one with a complete failure of the cavity. The geometric characteristics of the subsidence trough (max. vertical displacement, width, volume, the maximum slope), the volume of collapsed soil are some parameters that are used to appreciate the relevance of the model.

## 4.1 *The stable state*

The displacements observed near the surface are very small for the experimental test : less than 0.2mm determined by the digital imagery method. The displacements calculated with the numerical model are much more important : the maximum is close to 5mm. The same observation can be done with the maximum deflexion on the roof of the cavity. The digital imagery gives 0.3mm for the experimental test, while the numerical model presents a maximum approximately equivalent to 5mm (the displacement observed on the ground surface).
This huge difference can be explained at least partially. To introduce the cohesion in the numerical model, contact bonds were used. However a characteristic of this type of bond is to allow some rotational movement between the two particles. No bending moment is transmitted by this bond. It is quite different from the use of the aqueous glue in the analogical cohesive soil. Thus a certain internal freedom of deformation/adaptation in the hard soil layer has as consequence a bending stiffness much weaker than what we would like to model. As improvement for the future, the use of Parallel Bond in PFC would be more interesting, because it allows transmitting a bending moment between two particles.
Figure 9 shows the development of the contact forces between the particles.

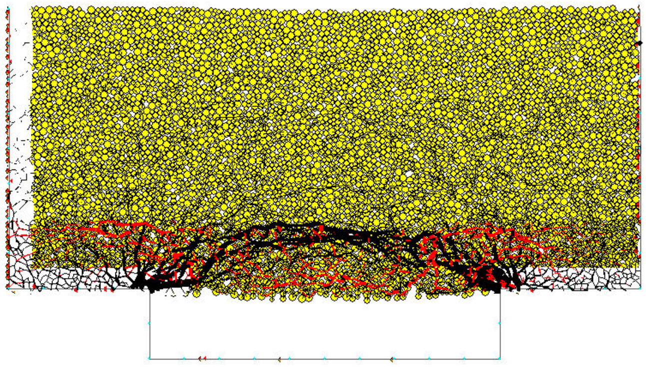

Fig. n°9 : Development of the compression (black) and tension force (red) when the cavity is wide open.

Arching phenomenon can be seen in black, taking support on the edges. This is the localization of the most important compression areas. On the opposite, the tension is mainly located in the lower part of the roof of the cavity and in the upper part of the beam on support (in dark grey). There is no important stress in the other parts of the soil mass. The frictional soil is not submitted to important stresses.

## *4.2 The failure*

The failure state is important because it corresponds to the more important stress for a building standing on the ground. To be able to forecast the deformations of the soil mass with a good reliability is fundamental.
First the displacements on the soil surface will be compared. Figure 10 shows the two subsidence troughs. The correlation is good, even though the failure mechanism is not exactly the same between the experimental test and the computation (cf. Figure 8).

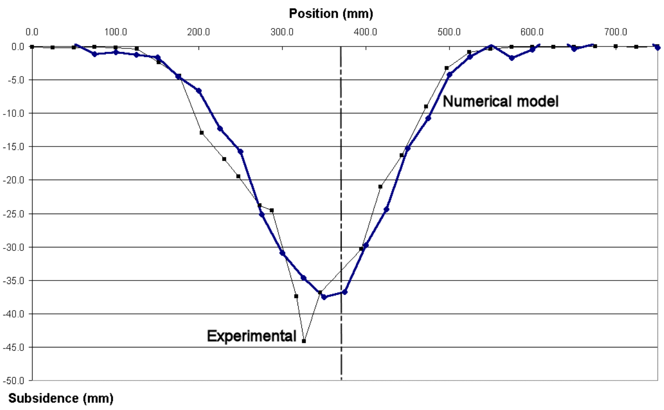


Fig n°10 : Comparison of the experimental and calculated subsidence troughs.

The width of the concerned area is very similar in the two cases. A small difference can be seen on the value of the maximum settlement : 43mm (1,72m in full scale) for the experimental test and 38mm (1,52m in full scale) for the numerical model. It is a good result for the FLAC-PFC coupled approach, even though it would be necessary to confirm these observations with other test results.
The slopes of the two curves are very close, around 40-45% for the physical model and 37-40% for the numerical approach. The main difference is located on the left part of the trough. It is exactly where we have noticed the difference of failure mechanism between the two tests.

The last thing that may be studied is the volume of both subsidence area and collapsed soil in the cavity. As it clearly appears on Figure 10, the trough volumes are very similar: $435cm^3$ for the numerical result versus $443cm^3$, less than 2% difference.
For the collapsed volume of soil, it was not straight forward to determine an accurate volume. In fact, we determined the volume of soil that had fallen into the cavity, not the volume of soil that had fallen into the cavity plus the volume of soil that moved to at this place. For the experimental model, a volume of $642cm^3$ is found while for the FLAC-PFC approach, it is $450cm^3$. The difference is very important, more than 30% less. The reason is that for the experimental result, the analogical soil is considered as bidimensionnal. It is true as far as the rods stay collinear. Figure 11 shows very well what actually happened.

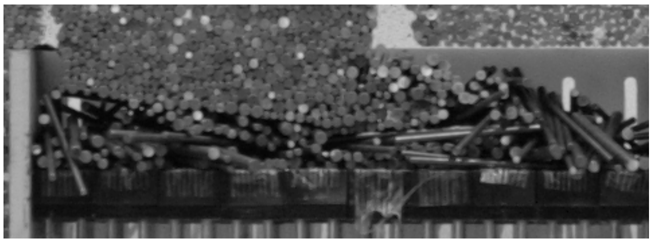

Fig. n°11 : Disorder with the analogical soil.

Thus the imagery processing gives a "false" volume for the collapsed soil. It is very similar to the expansion phenomenon observed in real soil, but here with a value too much important compared to what would be expected.
With PFC, the particles are really bidimensionnal, so it is not possible to observe such thing.
We can determine an similar expansion coefficient taking account of these two values: $R = \frac{V_{soilcollapsed}}{V_{trough}}$

For the numerical model, K would be 1,03 while the experimental results yield a value of 1,45.

# 5 Conclusions

The double approach using an experimental model and a coupled FLAC-PFC model allows observing the creation of a sinkhole. They are very complementary. The physical model allows to represent a case of study and to determine it completely with a limited set of parameters.
The numerical model using a coupled approach is first calibrated on these results and shows promising results. Nevertheless it has to be improved in the modelling of the cohesive layer and to model a small and simple building like the one used in the experimental method. Further developments will include the analysis of several real cases, less better known and the evaluation of the relevance of the numerical method.

# References

[BAZANT, 2004] BAZANT, Z. (2004). Introduction aux effets d'échelles sur la résistance des structures. *Hermes-Lavoisier*, Paris, 255p.

[CAUDRON et al., 2003] CAUDRON M., MATHIEU P., EMERIAULT F. and AL HEIB M. (2003). Effondrement de cavités souterraines et interaction avec les ouvrages en surface : approche expérimentale sur modèle analogique bidimensionnel, *Journées Nationales de la Géotechnique et de la Géologie pour l'Ingénieur*, juin 2003, 435-442.

[DECK et al., 2002] DECK O., AL HEIB M., GUENIFFREY Y., WOJTKOWIAK F. and HOMAND F. (2002). Méthode de prévision des dégradations des structures bâties en zone d'affaissement minier. *Revue Française de Géotechnique*, 100:15-33.

[DEHOUSSE et ARNOULD, 1971] DEHOUSSE et ARNOULD (1971). Les modèles réduits de structure en Génie Civil. *DUNOD*, 183p.

[DOLZHENKO, 2002] DOLZHENKO, N. (2002). Etude expérimentale et numérique de modèle réduit bidimensionnel du creusement d'un tunnel. Développement d'une loi de comportement spécifique. *PhD Thesis*, Institut National des Sciences Appliquées de Lyon. 198p.

[ITASCA, 2004] ITASCA Consulting Group (2004). $PFC_{2D}$ 3.1 Manual provided with the $PFC_{2D}$ code.

[NAKAI et al., 1997] NAKAI T., XU L. and YAMAZAKI H. (1997). 3d and 2d model tests and numerical analyses of settlements and earth pressures due to tunnel excavation. *Soil and Foundations*, 37:31-42.

[PECK, 1969] PECK (1969). Deep excavations and tunnelling in soft ground, *Proceedings of the 7$^{th}$ International Conference on Soil Mechanics Foundation Engineering*, Mexico, 3:225-290.

[SCHNEEBELI, 1956] SCHNEEBELI (1956). Une mécanique pour les terres sans cohésion. *Compte Rendu de l'Académie des Sciences*, 243:2647-2673.

[TOUCHAL et al., 1997] TOUCHAL S., MORESTIN F. and BRUNET M. (1997). Mise au point d'une nouvelle méthode de mesure de champs de déformations par corrélation directe d'images numériques, *European Journal of Mechanical Engineering*, BSMEE N°4, 42:197-204.

[VEZOLE, 2002] VEZOLE, P. (2002). Prise en compte des vides de dissolution de gypse dans les projets de construction. *Revue Française de Géotechnique*, 100:71-74.

[WHITE et al., 2003] WHITE D., TAKE W. and BOLTON M. (2003). Soil de formation measurement using particle image velocimetry (PIV) and photogrammetry. *Geotechnique*, 53:619-631.